Vibrationally resolved photoelectron spectra of $CuCN^-$ and $AgCN^-$ and *ab initio* studies of the structure and bonding in CuCN

Alexander I. Boldyrev
Department of Chemistry and Biochemistry, Utah State University, Logan, Utah 84322-0300

Xi Li and Lai-Sheng Wang
Department of Physics, Washington State University, Richland, Washington 99352 and W. R. Wiley Environmental Molecular Sciences Laboratory, Pacific Northwest National Laboratory, MS K8-88, P.O. Box 999, Richland, Washington 99352

(Received 27 October 1999; accepted 3 December 1999)

Vibrationally resolved photoelectron spectroscopy is combined with *ab initio* calculations to investigate the structure and chemical bonding in CuCN, $CuCN^-$, AgCN, and $AgCN^-$. The photoelectron spectra were measured at two photon energies, 532 and 355 nm and only detachment to the ground state of the neutral was observed at both detachment energies. The adiabatic electron affinity and metal-C vibrational frequency were obtained to be 1.466 (0.010) eV and 480(30) cm^{-1}, 1.588 (0.010) eV and 390(30) cm^{-1} for CuCN and AgCN, respectively. In the *ab initio* calculations, both CuCN and $CuCN^-$ were found to have linear $C_{\infty V}$ structures. Isocyanide CuNC and $CuNC^-$ were found to be 10.7 and 6.5 kcal/mol [at the CCSD(T)/6-311+G(3d)//CCSD(T)/6-311+G* level of theory] higher in energy. Cyclic structures were found to be transition states for the cyanide–isocyanide isomerization. The calculated electron binding energies and vibrational frequency are in good agreement with the experimental measurements. The combined experimental and theoretical efforts allow us to elucidate the structures of CuCN and $CuCN^-$, and the nature of their chemical bonding. © *2000 American Institute of Physics.* [S0021-9606(00)01808-0]

I. INTRODUCTION

The cyanide anion (CN^-) is isoelectronic to CO and its chemical bonding to metal surface is of considerable interest. To understand the nature of the bonding of the cyanide ligand to metal surfaces, simple XCN molecules have been considered and a variety of structures have been found. In X–CN, CN is σ-coordinated to X through the carbon atom. A σ-coordination through the N end to X is also possible, forming the linear isocyanide X–NC species. Furthermore, a π-bonded complex to X is also possible, giving a cyclic structure.

The alkali metal cyanides were among the first nonrigid molecules for which *ab initio* calculations were used to establish a flattened potential energy surface.[1] *Ab initio* studies revealed various potential surface shapes among the different alkali metal cyanides. For example, the global minimum on the potential energy surface of lithium cyanide was found to be the linear isocyanide configuration LiNC.[1–6] This result was confirmed by experimental infrared spectra of lithium isocyanide trapped in inert solid matrices[7] and gas-phase rotational spectra of LiNC.[8] However, *ab initio* studies showed sodium cyanide to be a T-shape, bridged structure,[6,9,10] which was also confirmed by experimental rotational constants of NaCN.[11,12] Similar T-shape structures were found for KCN[6,9,13–16] and RbCN.[17] For alkali earth monocyanides, *ab initio* calculations predicted that they are actually monoisocyanides (X–NC) for the entire family of molecules from Be to Ba.[18] These *ab initio* results have also been confirmed by experimental spectroscopic studies.[19–23] For Al cyanide systems, *ab initio* calculations also predicted the linear isocyanide Al–NC isomer to be more stable than the linear Al–CN isomer by several kcal/mol.[24–28] These theoretical predictions have again been confirmed by spectroscopic[27–31] and thermodynamic investigations.[32,33]

However, when less electropositive atoms react with CN, the most stable structure is X–CN. For example, *ab initio* calculations have predicted the linear B–CN isomer to be more stable than the isocyanide B–NC isomer by 12.4 kcal/mol.[3] All *ab initio* studies of transition metal cyanides[34–38] have predicted that the X–CN structures are several kcal/mol more stable than the isocyanide X–NC structures. A recent photoelectron spectroscopic study[39] of palladium cyanide anion also suggested that it has the X–CN structure for both the anion and neutral species.

When X=H, the global minimum is the well-known linear hydrogen cyanide molecule HCN. The linear isocyanide configuration HNC is a local minimum lying 11.2 kcal/mol higher than the global minimum.[40] The two minima are separated by a high barrier of 23.7 kcal/mol whose apex corresponds to a triangular configuration so that at low temperatures both isomers exist.

It seems that more covalent bonding between X and CN favors the linear cyanide structure, while more ionic bonding favors the linear isocyanide structure and in the extreme ionic cases even cyclic structures are possible. Transition metals are expected to form an ionic bond with CN rather than a covalent one, yet in all previous *ab initio* calculations the cyanide isomers were predicted to be more stable. However, these were based on the SCF, CASSCF, or SDCI levels of theories, which did not take into account much of the

dynamic electron correlation. For transition metal molecules the cyanide and isocyanide structures are very close in energy and therefore more accurate calculations are needed to make more definite conclusions about their relative stabilities.

Experimental studies of the transition metal cyanide molecules are also rare and very limited experimental data exist about these species. In the current work, photoelectron spectroscopy is combined with *ab initio* calculations to investigate the structure and chemical bonding in $CuCN^-$, CuCN, $AgCN^-$ and AgCN. A well-resolved vibrational progression was observed in the photoelectron spectra of $CuCN^-$ and $AgCN^-$. The measured vibrational frequencies and electron binding energies are used for comparison with the *ab initio* calculations. Indeed we found that all these species exist as the linear cyanide structures.

II. EXPERIMENT

The experiments were performed using a magnetic-bottle photoelectron apparatus with a laser vaporization cluster source. Details of the apparatus have been published previously.[41,42] The $CuCN^-$ and $AgCN^-$ anions were produced by laser vaporization of the respective pure metal target with a helium carrier gas containing 5% N_2. Various metal nitride clusters were produced and the XCN^- anions were formed due to carbon impurities in the targets or on the surfaces inside the cluster nozzle. The clusters formed inside the nozzle were entrained in the carrier gas and underwent a supersonic expansion. The anions were extracted from the cluster beam perpendicularly into a time-of-flight (TOF) mass spectrometer. The anions of interest were selected by a mass-gate and subsequently decelerated before crossing with a detachment laser beam in the interaction zone of the magnetic-bottle photoelectron analyzer. Two detachment photon energies at 2.331 (532 nm) and 3.496 (355 nm) eV from a *Q*-switched Nd:YAG laser were used in the current experiments. Photoelectrons were collected with nearly 100% efficiency by the magnetic-bottle and analyzed in a 3.5-m long electron TOF tube. The apparatus was operated at 10 Hz repetition rate. The electron kinetic energy scale was calibrated using the known spectrum of Cu^-. The apparatus has an electron energy resolution of about 20–25 meV for 1 eV electron.

III. COMPUTATIONAL METHODS

In the theoretical study, we focused on the Cu cyanide systems and expected that the bonding in the Cu and Ag systems would be similar. We initially optimized the geometries of CuCN, $CuCN^-$, CuNC, and $CuNC^-$, employing analytical gradients with polarized split-valence basis sets (6-311+G*)[43–45] using the hybrid method, which includes a mixture of Hartree–Fock exchange with density functional exchange correlation (B3LYP).[46–48] Then, the geometries were reoptimized using MP2/6-311+G* level of theory.[49] The geometries were further refined using the CCSD(T) method[50–52] and the same basis sets. Finally, the energies of the lowest-energy structures were refined using the CCSD(T) level of theory and the more extended 6-311+G(3*d*) basis sets. All core electrons (Cu $1s-3p$, C $1s$, and N $1s$) were kept frozen; the Cu *d* electrons were not frozen and were included in treating the electron correlation at the MP2 and CCSD(T) levels of theory. Effective atomic charges were calculated using natural population analysis (NPA).[53,54] Because NPA analysis is not available for the CCSD(T) method, we used QCISD method instead.[55] All calculations were performed using the GAUSSIAN-98 program.[56]

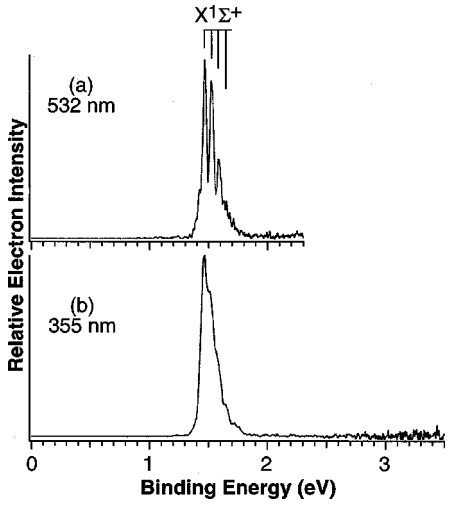

FIG. 1. Photoelectron spectra of $CuCN^-$ at (a) 532 nm (2.331 eV) and (b) 355 nm (3.496 eV). The vertical lines indicate vibrational features.

IV. EXPERIMENTAL RESULTS

Figure 1 shows the photoelectron spectra of $CuCN^-$ at 532 and 355 nm. A well-resolved vibrational progression was observed in the 532 nm spectrum, yielding an adiabatic detachment energy of 1.466 (0.010) eV and a vibrational frequency of 480 (30) cm^{-1}. Hot band features were discernible in the lower energy side of the 532 nm spectrum [Fig. 1(a)] but could not be resolved, probably because the anion has a much smaller vibrational frequency. At 355 nm, no new features were observed at higher binding energies.

Figure 2 shows the photoelectron spectra of $AgCN^-$ at 532 and 355 nm. The 532 nm spectrum of $AgCN^-$ is very similar to that of $CuCN^-$ with a well-resolved vibrational progression starting at 1.588 eV, except that an extra and very week feature (X') near 1.12 eV was also present. The well-resolved progression yielded an adiabatic detachment energy of 1.588 (0.010) eV and a vertical detachment energy of 1.636 (0.010) eV, and a vibrational frequency of 390 (20) cm^{-1}. The 355 nm spectrum of $AgCN^-$ was also similar to that of $CuCN^-$ except that several more weak features were observed at higher binding energies.

The weak features in the $AgCN^-$ spectra depended on the source conditions to some degree, but could not to be completely eliminated. Under certain source conditions, similar weak features were also observed in the $CuCN^-$ spectra. Thus we tentatively concluded that these weak features were due to either minor isomers or electronically excited states of the anions. The observed spectroscopic parameters of the main transitions for $CuCN^-$ and $AgCN^-$ are summarized in Table I.

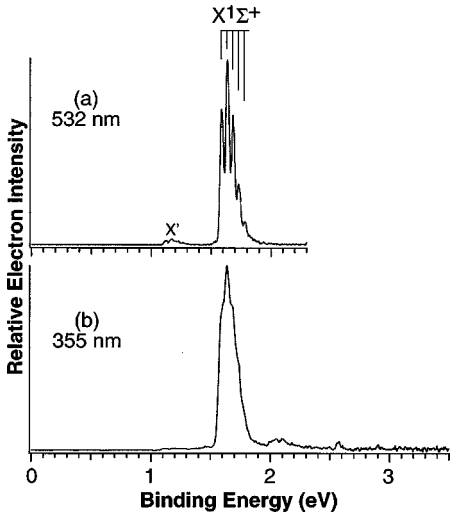

FIG. 2. Photoelectron spectra of $AgCN^-$ at (a) 532 nm (2.331 eV) and (b) 355 nm (3.496 eV). The vertical lines indicate vibrational features.

V. THEORETICAL RESULTS

To understand the structure and bonding of the XCN^- species and to interpret the observed spectral transitions, we carried out *ab initio* calculations on two possible isomers of $CuCN^-$ and $CuNC^-$ and their respective neutrals. It was too expensive to perform calculations of similar accuracy on the $AgCN^-$ systems. However, we expected that the structure and bonding in the two systems should be similar.

Our theoretical results for CuCN, CuNC, $CuCN^-$, and $CuNC^-$ are summarized in Tables II–IV. We should point out that all harmonic frequencies in the tables are not scaled.

A. CuCN and CuNC

At all three levels of theory, B3LYP/6-311+G*, MP2/6-311+G*, and CCSD(T)/6-311+G*, the global minimum of CuCN was found to have a linear singlet $C_{\infty V}$ structure ($^1\Sigma^+, 1\sigma^2 2\sigma^2 1\pi^4 1\delta^4 3\sigma^2 4\sigma^2 2\pi^4 5\sigma^0$), as characterized in Table II. This result agrees with all previous *ab initio* calculations.[34–38] However, the detailed numerical results are quite different. The best previous results were obtained by Bauschlicher[35] at the SDCI level of theory using $(14s13p9d1f/7s7p4d1f)_{Cu}+(9s6p/4s3p)_{C,N}$ basis sets, which gave the following results: $R(\text{Cu–C})=1.90$ Å, $R(\text{C–N})=1.17$ Å, $\mu_e=8.41$ D, $\omega_2=360\,\text{cm}^{-1}$, and $D_e=4.14$ eV, compared with our results: $R(\text{Cu–C})=1.86$ Å, $R(\text{C–N})=1.18$ Å, $\mu_e=7.46$ D, $\omega_2=453\,\text{cm}^{-1}$, and $D_e=5.22$ eV (Table II). The main differences are that the Cu–C bond is shorter, the Cu–CN frequency and the Cu–CN dissociation energy are substantially higher in the current calculations, due to better treatment of electron correlation. The Cu–CN frequency obtained from the current theoretical study is in excellent agreement with the experimentally measured frequency of Cu–CN (Table I), confirming the accuracy of the current calculations.

At the same levels of theory, the isocyanide Cu–NC isomer, $C_{\infty V}$ ($^1\Sigma^+, 1\sigma^2 2\sigma^2 1\pi^4 1\delta^4 3\sigma^2 4\sigma^2 2\pi^4 5\sigma^0$), was found to be a local minimum, 10.7 kcal/mol (CCSD(T)/6-311+G(3*d*)) higher in energy.

The cyclic structure corresponds to a transition state on the intramolecular rotation of Cu^+ around the CN^- group (Table III). The height of the internal rotation barrier is only 4.4 kcal/mol at the B3LYP/6-311+G* level of theory and

TABLE I. Observed spectroscopic constants for $CuCN^-$ and $AgCN^-$.

	ADE (eV)	VDE (eV)	Vib. freq. (cm^{-1})
$CuCN^-$	1.466 (0.010)	1.466 (0.010)	480(30)
$AgCN^-$	1.588 (0.010)	1.636 (0.010)	390(20)

TABLE II. Calculated molecular properties of CuCN and CuNC.

$C_{\infty V}, {}^1\Sigma^+$	B3LYP/6-311+G*	MP2/6-311+G*	CCSD(T)/6-311+G*
	CuCN		
R(Cu–C), Å	1.853	1.826	1.863
R(C–N), Å	1.161	1.182	1.177
E_{tot}, a.u.	−1733.363 774	−1731.905 716	−1731.876 434
$\omega_1(\sigma)$, cm^{-1}	2249	2079	2159
$\omega_2(\sigma)$, cm^{-1}	465	479	453
$\pi_3(\sigma)$, cm^{-1}	251	245	225
Q(Cu)[b]	+0.684	+0.752	+0.739[a]
Q(C)[b]	−0.253	−0.345	−0.317[a]
Q(N)[b]	−0.430	−0.407	−0.422[a]
μ, D	7.158	7.470	7.457[a]
	CuNC		
R(Cu–N), Å	1.816	1.794	1.826
R(C–N), Å	1.177	1.191	1.189
E_{tot}, a.u.	−1733.345 854	−1731.884 213	−1731.859 092
$\omega_1(\sigma)$, cm^{-1}	2141	2050	2084
$\omega_2(\sigma)$, cm^{-1}	484	494	475
$\omega_3(\pi)$, cm^{-1}	147	124	119
Q(Cu)[b]	+0.820	+0.884	+0.856
Q(N)[b]	−0.982	−0.981	−0.992
Q(C)[b]	+0.162	−0.096	+0.136
μ, D	7.207	7.966	7.562

[a]At the QCISD/6-311+G(3*d*) level of theory using CCSD(T)/6-311+G* geometry.
[b]Effective atomic charge in $|e|$.

TABLE III. Calculated molecular properties of the transition states of CuNC and CuNC−.

$C_s, {}^1A'$	B3LYP/6-311+G*	MP2/6-311+G*
	CuNC(TS)	
R(Cu–N), Å	1.878	1.822
R(C–C), Å	2.365	2.562
R(C–N), Å	1.187	1.202
E_{tot}, a.u.	−1733.338 840	−1731.881 294
$\omega_1(a')$, cm^{-1}	2029	1942
$\omega_2(a')$, cm^{-1}	497	550
$\omega_3(a')$, cm^{-1}	123 *i*	117 *i*
	$CuNC^-$(TS)	
R(Cu–N), Å	2.195	2.185
R(Cu–C), Å	2.186	2.069
R(C–N), Å	1.181	1.202
E_{tot}, a.u.	−1733.396 296	−1731.925 028
$\omega_1(a')$, cm^{-1}	2069	1947
$\omega_2(a')$, cm^{-1}	254	298
$\omega_3(a')$, cm^{-1}	158 *i*	143 *i*

TABLE IV. Calculated molecular properties of $CuCN^-$ and $CuNC^-$.

$C_{\infty V}, {}^2\Sigma^+$	B3LYP/6-311+G*	MP2/6-311+G*	CCSD(T)/6-311+G*
		CuCN	
R(Cu–C), Å	1.937	1.878	1.932
R(C–N), Å	1.167	1.185	1.181
E_{tot}, a.u.	−1733.420 168	−1731.949 320	−1731.923 412
$\omega_1(\sigma)$, cm^{-1}	2186	2246	2117
$\omega_2(\sigma)$, cm^{-1}	360	399	367
$\omega_3(\pi)$, cm^{-1}	223	236	216
Q(Cu)[a]	−0.304	−0.373	−0.354
Q(C)[a]	−0.098	−0.077	−0.070
Q(N)[a]	−0.598	−0.564	−0.576
		$CuNC^-$	
R(Cu–N), Å	1.921	1.870	1.911
R(C–N), Å	1.174	1.191	1.187
E_{tot}, a.u.	−1733.409 640	−1731.934 777	−1731.912 778
$\omega_1(\sigma)$, cm^{-1}	2139	2033	2076
$\omega_2(\sigma)$, cm^{-1}	354	376	361
$\omega_3(\pi)$, cm^{-1}	151	141	135
Q(Cu)[a]	−0.020	−0.029	−0.013
Q(C)[a]	−0.961	−0.933	−0.965
Q(C)[a]	−0.019	−0.062	−0.026

[a]Effective atomic charge in $|e|$.

1.8 kcal/mol at the MP2/6-311+G* level of theory relative to the CuNC isomer.

B. $CuCN^-$ and $CuNC^-$

At all three levels of theory, B3LYP/6-311+G*, MP2/6-311+G*, and CCSD(T)/6-311+G*, the global minimum of Cu–CN^- was also found to have a linear structure with a doublet ground state, $C_{\infty V}$ $({}^2\Sigma^+, 1\sigma^2 2\sigma^2 1\pi^4 1\delta^4 3\sigma^2 4\sigma^2 2\pi^4 5\sigma^1)$, characterized in Table IV. At the same levels of theory, the isocyanide (Cu–NC^-), $C_{\infty V}$ $({}^2\Sigma^+, 1\sigma^2 2\sigma^2 1\pi^4 1\delta^4 3\sigma^2 4\sigma^2 2\pi^4 5\sigma^1)$, was found to be a local minimum 6.5 kcal/mol (CCSD(T)/6-311+G(3d)) higher in energy. The cyclic structure again corresponds to a transition state on the intramolecular rotation of Cu^+ around the CN^- group. The height of the internal rotation barrier is 8.4 kcal/mol at the B3LYP/6-311+G* level of theory and 6.1 kcal/mol at the MP2/6-311+G* level of theory relative to the Cu–NC^- isomer.

The CuCN neutral is very stable towards dissociation as one can expect based on the ionic bonding. The stability of the $CuCN^-$ anion drops substantially since the extra electron occupies the 5σ MO, which is primarily of Cu 4s character, substantially reducing the ionic bond strength. The dissociation energies were calculated to be $\Delta E = 5.22$ eV for $CuCN(C_{\infty V}, {}^1\Sigma^+) \rightarrow CN(C_{\infty V}, {}^2\Sigma^+) + Cu({}^2S)$ and $\Delta E = 1.74$ eV for $CuCN^-(C_{\infty V}, {}^2\Sigma^+) \rightarrow CN^-(C_{\infty V}, {}^2\Sigma^+) + Cu({}^2S)$ [both at the CCSD(T)/6-311+G(3d) level of theory]. The substantial increase of the Cu–C bondlength and decrease of the Cu–C vibrational frequency (ω_2, Table IV) are also consistent with the considerable weakening of the Cu–CN bonding in the anion.

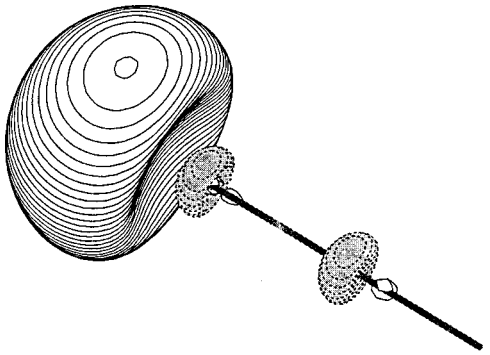

FIG. 3. Molecular orbital picture (Ref. 57) showing the Cu 4s character of the HOMO (5σ) of $CuCN^-$.

VI. DISCUSSION

Neutral CuCN is a closed-shell molecule $({}^1\Sigma^+)$ and can be viewed as Cu^+CN^- with an electron configuration: $1\sigma^2 2\sigma^2 1\pi^4 1\delta^4 3\sigma^2 2\pi^4 5\sigma^0$. In the anion, the extra electron enters the 5σ LUMO. Since the 5σ MO is predominantly of Cu 4s character (Fig. 3), the anion $CuCN^-$ can be viewed as a neutral Cu atom interacting with a closed-shell CN^-. Thus the bonding between Cu and CN moiety is considerably reduced in the anion. Indeed, our calculations (Table II) indicated that in Cu–CN the atomic charge on Cu is close to +1 (+0.74) and the charge on CN is close to −1 (−0.74). In the anion, the additional electron almost completely goes to Cu with some additional polarization of the CN^- group (electron density on CN^- is shifted towards the nitrogen atom), as shown in Fig. 3. The Cu–CN bond in the anion is elongated by 0.07 Å and its ω_2 vibrational frequency is lowered by 86 cm^{-1} (by 19%).

The observed photoelectron spectrum (Fig. 1) is consistent with this bonding picture. The photoelectron spectrum should correspond to removal of the 5σ electron in $CuCN^-$. The observed vibrational progression indeed suggests that there is a considerable geometry change upon detachment of an electron from $CuCN^-$ and a considerable increase of the ν_2 vibrational frequency [as inferred from the unresolved hot band feature, Fig. 1(a)]. The calculated electron detachment energies of $CuCN^-$ are shown in Table V. It should be noted that the VDE and ADE given in Table V are calculated with a larger basis set [CCSD(T)/6-311-G(3d)] than the geometry optimizations, which are done at the CCSD(T)/6-311+G* level of theory. The 1.34 eV ADE obtained at the higher level of theory represents a 0.05 eV improvement relative to the value of 1.29 eV at the CCSD(T)/6-311

TABLE V. Comparison of calculated and experimental electron detachment processes of $CuCN^-$.

	Experiment VDE (eV)	Experiment ADE (eV)	Electron detachment from MO	Theory VDE[a] (eV)	Theory ADE[a] (eV)
$CuCN^-$	1.466 (10)	1.466 (10)	5σ	1.37	1.34
$CuNC^-$			5σ	1.57	1.52

[a]At the CCSD(T)/6-311+G(3d) level of theory using CCSD(T)/6-311+G* geometry. Zero point energy correction is not included.

+G* level of theory (Tables II and IV). Even with the improved level of theory the calculated VDE and ADE of $CuCN^-$ are still somewhat lower than the experimental values. Calculations of electron affinities of such systems certainly require large basis sets, which are beyond the scope of the current study. Our calculations of the Cu^- anion have shown that our level of theory yielded an electron affinity for Cu of 1.067 eV, compared to the experimental value of 1.235(5) eV.[56] Therefore, our calculated electron binding energies for $CuCN^-$ should be considered with similar accuracy. They are likely to be underestimating the true values. If we add the difference between the true and calculated electron affinity of Cu to our calculated binding energies for $CuCN^-$, we obtain much better agreement with the experimental values. Zero point energies are not calculated at the CCST(D)/6-311-G(3*d*) level of theory, and thus are not included in the calculations of the ADE's given in Table V. However, the zero point energy corrections are expected to be negligible. At the CCST(D)/6-311-G* level of theory, the zero point energies are 4.377 and 4.167 kcal/mol for CuCN and $CuCN^-$, respectively, resulting in a correction of less than 0.01 eV for the ADE. This is negligible considering the accuracy of the current calculations.

We can rule out the possibility that the isocyanide $CuNC^-$ was responsible for our observed spectra in Fig. 1 based on both energetic ground and the calculated binding energies, even though the observed vibrational frequency can be assigned to the ν_2 mode of either CuCN or CuNC because they are very similar (Table II). According to our best calculations, the linear cyanide CuCN and $CuCN^-$ structures are more stable than the linear isocyanide isomers CuNC and $CuNC^-$ by 10.7 and 6.5 kcal/mol, respectively. Furthermore, the potential barriers between the isocyanide structure and the cyclic transition state are relatively low for both the neutral and the anion. One would expect very little population of the isocyanide $CuCN^-$ isomer in our beam. Our calculated electron binding energies for the $CuCN^-$ isomer are also in very good agreement with the experimental values (Table V), taking into account the fact that our current calculations tended to underestimate the binding energies, as discussed above. We can exclude $CuNC^-$ as a candidate rather firmly, because the calculated binding energies for this isomer (Table V) are already higher than the experimental values. If $CuNC^-$ were present in our beam, it should appear as weak features at a higher binding energy than the observed features for $CuCN^-$. Our data clearly suggest that no measurable amount of $CuNC^-$ was present in our beam.

The main features of the $AgCN^-$ spectra are almost identical to that of the $CuCN^-$ spectra, except that $AgCN^-$ has a higher electron binding energy and gives a lower vibrational frequency. The bonding in AgCN is expected to be similar to that in CuCN. We can expect that the extra electron in $AgCN^-$ also occupies an orbital of mainly Ag 5*s* character. The increased electron affinity of AgCN is also anticipated based on the higher electron affinity of Ag (1.302 eV), relative to that of Cu (1.235 eV).[56] However, extra weak features were observed in the $AgCN^-$ spectra, as shown in Fig. 2. The weak higher binding energy feature near 2 eV observed in Fig. 2(b) might be due to the isocyanide $AgNC^-$ isomer, although that feature did not appear in the 532 nm spectrum [Fig. 2(b)], suggesting that this isomer was only present under certain experimental conditions. However, the lower binding energy feature (X′) was still puzzling. It cannot be due to the $AgNC^-$ isomer, because it was expected to have a higher binding energy. In addition, this feature was stronger in Fig. 2(a) where the 2 eV feature, observed in Fig. 2(b) and attributed to the $AgNC^-$ isomer, was not present, suggesting that the X′ feature and the 2 eV feature have different origins. We tentatively attributed the X′ feature to an excited anion state of $AgCN^-$. Therefore, there seems to be experimental evidence that very weak isocyanide $AgNC^-$ might be present in our beam. Unfortunately, accurate theoretical calculations of the silver cyanide systems would require inclusion of relativistic effects and are beyond this study. Further theoretical studies are warranted for these systems. In particular, the isocyanide $AgNC^-$ isomer may be more stable relative to $CuNC^-$ or that the barrier between the $AgNC^-$ and the $AgCN^-$ isomers are significantly larger, making it easier to be observed experimentally.

VII. CONCLUSIONS

We report vibrationally resolved photoelectron spectra of $CuCN^-$ and $AgCN^-$ and a detailed theoretical investigation of $CuCN^-$ and CuCN and their isomers. Vibrational frequencies and electron affinities of CuCN and AgCN were obtained for the first time in the gas phase. Our theoretical calculations predicted that CuCN and $CuCN^-$ both have $C_{\infty V}$ linear structures as their global minima with the isocyanide isomers higher in energy. The agreement between the calculated and experimental spectroscopic parameters confirms the linear structures of CuCN and $CuCN^-$.

ACKNOWLEDGMENTS

The theoretical work was done at Utah State University. The experimental work done in Washington is supported by the National Science Foundation (CHE-9817811). The experiment was performed at the W. R. Wiley Environmental Molecular Sciences Laboratory, a national scientific user facility sponsored by DOE's Office of Biological and Environmental Research and located at Pacific Northwest National Laboratory, which is operated for DOE by Battelle under Contract No. DE-AC06-76RLO 1830. L.S.W. is an Alfred P. Sloan Foundation Research Fellow.

[1] E. Clementi, H. Kistenmacher, and H. Popkie, J. Chem. Phys. **58**, 2460 (1973).
[2] A. I. Boldyrev, *et al.* Russ. J. Inorg. Chem. **24**, 341 (1979).
[3] L. T. Redmon, G. D. Purvis III, and R. J. Bartlett, J. Chem. Phys. **72**, 986 (1980).
[4] R. Essers, J. Tennyson, and P. E. S. Wormer, Chem. Phys. Lett. **89**, 223 (1982).
[5] L. Adamowicz and C. I. Frum, Chem. Phys. Lett. **157**, 496 (1989).
[6] A. Dorigo, P. v. R. Schleyer, and P. Hobza, J. Comput. Phys. **15**, 322 (1994).
[7] Z. K. Ismail, R. H. Hauge, and J. L. Margrave, J. Chem. Phys. **57**, 5137 (1972).
[8] J. J. van Vaals, W. L. Meerts, and A. Dymanus, Chem. Phys. **82**, 385 (1983).
[9] M. L. Klein, J. D. Goddard, and D. G. Bounds, J. Chem. Phys. **75**, 3909 (1981).

[10] C. J. Marsden, J. Chem. Phys. **76**, 6451 (1982).
[11] J. J. van Vaals, W. L. Meerts, and A. Dymanus, J. Chem. Phys. **77**, 5245 (1982).
[12] J. J. van Vaals, W. L. Meerts, and A. Dymanus, Chem. Phys. **86**, 147 (1984).
[13] P. E. S. Wormer and J. Tennyson, J. Chem. Phys. **75**, 1245 (1981).
[14] P. Kuijpers, T. Torring, and A. Dymanus, Chem. Phys. Lett. **42**, 423 (1976).
[15] T. Torring *et al.*, J. Chem. Phys. **73**, 4875 (1980).
[16] J. J. van Vaals, W. L. Meerts, and A. Dymanus, J. Mol. Spectrosc. **106**, 280 (1984).
[17] E. van Leuken, G. Brocks, and P. E. S. Wormer, Chem. Phys. **110**, 365 (1986).
[18] C. W. Bauschlicher, Jr., S. R. Langhoff, and H. Partridge, Chem. Phys. Lett. **115**, 124 (1985).
[19] K. Kawaguchi, E. Kagi, T. Hirane, S. Takano, and S. Saito, Astrophys. J. **406**, L39 (1993).
[20] C. J. Whitham, B. Soep, J.-P. Visticot, and K. Keller, J. Chem. Phys. **93**, 991 (1980).
[21] M. Douay and P. F. Bernath, Chem. Phys. Lett. **174**, 230 (1990).
[22] T. C. Steimle, D. A. Fletcher, K. Y. Jung, and C. T. Scurlock, J. Chem. Phys. **97**, 2909 (1992).
[23] C. T. Scurlock, T. C. Steimle, R. D. Suenram, and F. J. Lovas, J. Chem. Phys. **100**, 3497 (1994).
[24] B. Ma, Y. Yamaguchi, and H. F. Schaefer III, Mol. Phys. **86**, 1331 (1995).
[25] S. Petrie, Mon. Not. R. Astron. Soc. **282**, 807 (1996).
[26] S. Petrie, J. Phys. Chem. **100**, 11581 (1996).
[27] D. V. Lanzisera and L. Andrews, J. Phys. Chem. A **101**, 9660 (1997).
[28] M. Fukushima, Chem. Phys. Lett. **283**, 337 (1998).
[29] J. S. Robinson, A. J. Apponi, and L. M. Ziurys, Chem. Phys. Lett. **278**, 1 (1997).
[30] K. A. Walker and M. C. Gerry, Chem. Phys. Lett. **278**, 9 (1997).
[31] I. Gerasimov, X. Yang, and P. J. Dagdigian, J. Chem. Phys. **110**, 220 (1999).
[32] K. A. Gingerich, Naturwissenschaften **24**, 646 (1967).
[33] G. Meloni and K. A. Gingerich, J. Chem. Phys. **111**, 969 (1999).
[34] D. G. Musaev and A. I. Boldyrev, Koord. Khim. **10**, 938 (1984).
[35] C. W. Bauschlicher, Jr. Surf. Sci. **154**, 70 (1985).
[36] C. J. Nelin, P. S. Bagus, and M. R. Philipott, J. Chem. Phys. **87**, 2170 (1987).
[37] X.-Y. Zhou, D.-H. Shi, and P.-L. Cao, Surf. Sci. **223**, 393 (1989).
[38] M. Tadjeddine, J. P. Flament, and A. Tadjeddine, J. Electroanal. Chem. **408**, 237 (1996).
[39] S. A. Klopcic, V. D. Moravec, and C. C. Jarrold, J. Chem. Phys. **110**, 8986 (1999).
[40] J. N. Murrell, S. Carter, and L. O. Halonen, J. Mol. Spectrosc. **93**, 307 (1982).
[41] L. S. Wang, H. S. Cheng, and J. Fan, J. Chem. Phys. **102**, 9480 (1995).
[42] L. S. Wang and H. Wu, in *Advances in Metal and Semiconductor Clusters, IV. Cluster Materials*, edited by M. A. Duncan (JAI, Greenwich, 1998), p. 299.
[43] A. D. McLean and G. S. Chandler, J. Chem. Phys. **72**, 5639 (1980).
[44] T. Clark, J. Chandrasekhar, G. W. Spitznagel, and P. v. R. Schleyer, J. Comput. Phys. **4**, 294 (1983).
[45] M. J. Frisch, J. A. Pople, and J. S. Binkley, J. Chem. Phys. **80**, 3265 (1984).
[46] R. G. Parr and W. Yang, *Density-Functional Theory of Atoms and Molecules* (Oxford University Press, Oxford, 1989).
[47] A. D. Becke, J. Chem. Phys. **96**, 2155 (1992).
[48] J. P. Perdew, *et al.* Phys. Rev. B **46**, 6671 (1992).
[49] R. Krishnan, J. S. Binkley, R. Seeger, and J. A. Pople, J. Chem. Phys. **72**, 650 (1980).
[50] J. Cizek, Adv. Chem. Phys. **14**, 35 (1969).
[51] G. D. Purvis III and R. J. Bartlett, J. Chem. Phys. **76**, 1910 (1982).
[52] G. E. Scuseria, C. L. Janssen, and H. F. Schaefer III, J. Chem. Phys. **89**, 7382 (1988).
[53] A. E. Reed and F. Weinhold, Chem. Rev. **88**, 889 (1988).
[54] J. A. Pople, M. Head-Gordon, and K. Raghavachari, J. Chem. Phys. **87**, 5968 (1987).
[55] GAUSSIAN 98 (revision A.7): M. J. Frisch, G. M. Trucks, H. B. Schlegel, G. E. Scuseria, M. A. Robb, J. R. Cheeseman, V. G. Zakrzewski, J. A. Montgomery, Jr., R. E. Stratmann, J. C. Burant, S. Dapprich, J. M. Millam, A. D. Daniels, K. N. Kudin, M. C. Strain, O. Farkas, J. Tomasi, V. Barone, M. Cossi, R. Cammi, B. Mennucci, C. Pomelli, C. Adamo, S. Clifford, J. Ochterski, G. A. Petersson, P. Y. Ayala, Q. Cui, K. Morokuma, D. K. Malick, A. D. Rabuck, K. Raghavachari, J. B. Foresman, J. Cioslowski, J. V. Ortiz, A. G. Baboul, B. B. Stefanov, G. Liu, A. Liashenko, P. Piskorz, I. Komaromi, R. Gomperts, R. L. Martin, D. J. Fox, T. Keith, M. A. Al-Laham, C. Y. Peng, A. Nanayakkara, C. Gonzales, M. Challacombe, P. M. W. Gill, B. G. Johnson, W. Chen, M. W. Wong, J. L. Andres, M. Head-Gordon, E. S. Replogle, and J. A. Pople, Gaussian, Inc., Pittsburgh PA, 1998.
[56] H. Hotop and W. C. Lineberger, J. Phys. Chem. Ref. Data **14**, 731 (1985).
[57] MO pictures were made using MOLDEN3.4 program. G. Schaftenaar, MOLDEN3.4, CAOS/CAMM Center, The Netherland, 1998.